RSC Advances

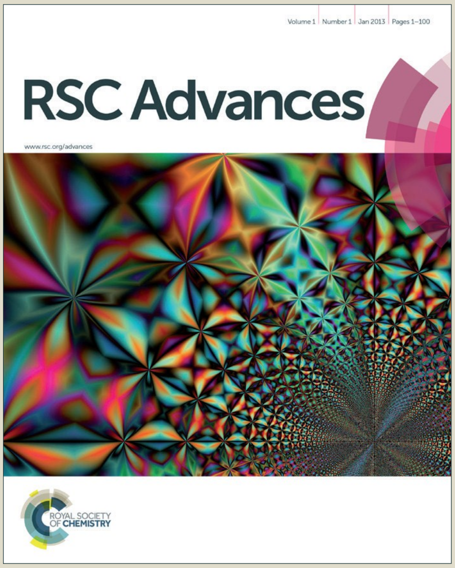

ROYAL SOCIETY OF CHEMISTRY

www.rsc.org/advances

Journal Name

COMMUNICATION

Fabrication of resist pattern based on plasma-polystyrene interaction

Received 00th January 20xx,
Accepted 00th January 20xx

DOI: 10.1039/x0xx00000x

www.rsc.org/

Ning Li, Lei Feng, Fei Teng, Yandong Wang, Feifei Wu, Xiangchao Yang and Nan Lu*

We report a straightforward method to fabricate resist patterns based on the interaction of oxygen plasma and polystyrene (PS) spheres within several minutes. The XPS results demonstrate that the resist pattern is formed by the PS fragments produced in the etching process. In the process, PS spheres not only serve as template for patterning, but also provide PS fragments to form the resist pattern. The ultrathin resist (UR) pattern can serve as a mask for dry etching with the selectivity of 21:1. In addition, the resist pattern can be used as template for selectively deposit silver nanoparticles because it can effectively block electrons.

Motivated by the demand for denser component integration in semiconductor industry, manufacturers and researchers have made considerable progress in high-resolution lithography techniques, such as photolithography,[1] extreme ultraviolet lithography,[2] electron beam lithography (EBL),[3] nanoimprint lithography (NIL),[4] nanosphere lithography (NSL),[5] etc. For all the techniques, to transfer pattern from resist layer to underlying substrate is one of the most important steps for the fabrication, which is usually completed by site-selective dry etching. In general, an ideal resist material is of high selectivity, high adhesion and enough mechanical stiffness.

The most conventional material is the carbon-based materials, such as polymethyl methacrylate,[4] PS,[6] SU-8,[7] etc, but some of them have lower selectivity and poorer adhesion, moreover, they may collapse during wet development due to poor stiffness.[8] In order to achieve a higher aspect ratio, some hard masks were proposed, such as hydrogen silsesquioxane (HSQ),[9] sputtered metal[10] and atomic layer deposition (ALD).[8, 11] HSQ is of relative high mechanical stability, which has been widely used in EBL,[12] NIL,[13] etc, however, its sensitivity to electron beam exposure is relative low,[14] and its hardness depends on the bake temperature and bake time.[9] Although metal film, like Au, Ag, Ni, and Cr, can be used as resist, multi-step process involved in resist patterning could limit its applications. The resist based on ALD is an ideal resist because it is highly stable and the thickness can be controlled in nanoscale, however, the fabrication process is complicated and time-consuming. For example, the substrate usually needs to be patterned and modified with hydroxyl groups in advance, and then the reaction of precursors and deposition are alternatively conducted, finally the resist are formed layer-by-layer.[15] So ALD deposition rate is very slow; moreover, the deposition process is complex and costly. Therefore, to develop a simple method for creating ideal resist patterns is highly needed.

Herein, inspired by the ALD process, we developed a straightforward and efficient method to create resist pattern on silicon (Si) within several minutes by using PS spheres as source of precursor.

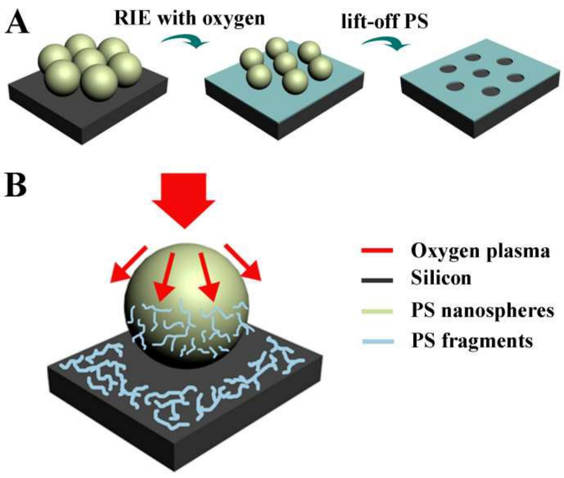

Fig. 1 (A) Procedure for the fabrication of resist pattern. (B) Schematic illustration of the formation for the resist pattern.

The fabrication procedure is shown in Fig. 1A. First, the monolayer of PS spheres was self-assembled on the Si slide.

State Key Laboratory of Supramolecular Structure and Materials, College of chemistry, Jilin University, Changchun 130012 (P.R. China).
E-mail: luenan@jlu.edu.cn

†Electronic Supplementary Information (ESI) available: Experimental details, SEM, and AFM data. See DOI: 10.1039/x0xx00000x

Then the assembled PS spheres were subjected to reactive ion etching (RIE) with oxygen. Here, the PS spheres not only served as the template for resist patterning, but also as the source of resist. The formation process of the resist pattern can be understood as Fig. 1B. The plasma flow contains ions, electrons, excited neutrals, radicals, and UV radiation. These highly reactive components lead to the chain scission of the PS molecules, generating the low-molecular-weight fragments. When the fragments with reactive radicals arrived on Si, they formed the polystyrene fragments layer. After lifting-off the spheres in toluene, the resist pattern was obtained.

We followed the transformation of PS spheres with scanning electron microscope (SEM). The 600 nm PS spheres were assembled into hexagonally packed arrangement (detailed in Fig. S1 of the ESI†). As revealed in Fig. 2A and B, the average diameter of PS spheres was accordingly decreased to 555 and 336 nm by conducting oxygen plasma etching for 3 and 9 min, respectively. Clearly, the surface of spheres became rougher as extending the etching duration, which was introduced by the inhomogeneous etching and the detachment of the PS fragments.

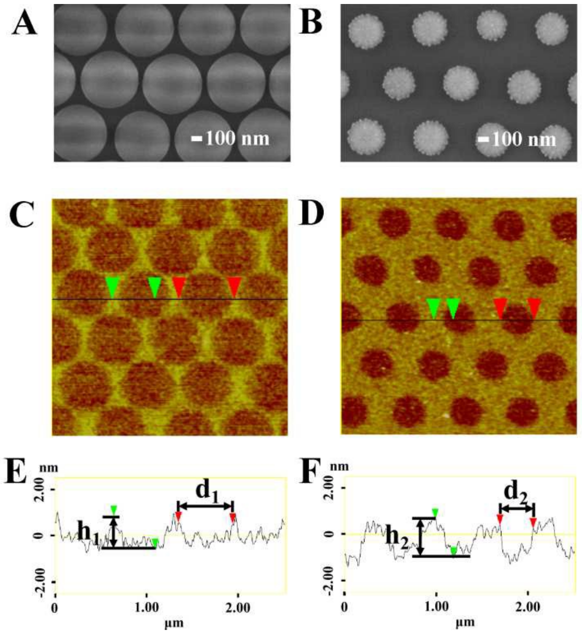

Fig. 2 SEM images of the PS spheres after oxygen etching for 3 min (A) and 9 min (B), respectively. AFM topography (C, D) and section analysis (E, F) of the UR pattern produced by 3 and 9 min oxygen etching, respectively.

After removing the PS spheres in toluene, the remained resist patterns were characterized with atomic force microscope (AFM). The topography images of the resist patterns created with different etching duration are shown in Fig. 2C and D. The section analysis (Fig. 2E and F) indicates that the average diameters of the holes on Si slides generated by 3 and 9 min etching are 593 nm (d_1) and 362 nm (d_2), respectively, which are slightly larger than that of the spheres. We attribute this to the anisotropic deposition caused by the horizontal movement of the plasma flow. This result shows that the features of the resist pattern can be controlled by tuning the size of spheres because they are template for the fragments deposition. As shown in Fig. 2E and F, the average thickness of the resist layer increases from 1.4 nm (h_1) to 1.7 nm (h_2) when the etching duration is extended from 3 to 9 min. The thickness of UR is just increased for 0.3 nm from 3min to 9min. During the formation of the UR, the deposition of PS fragments on silicon and the reduction of the UR take place at the same time during the etching process. The thickness of the UR decreases at a constant speed, but the increase speed of the thickness for the deposited PS fragments changes with the reduction of the PS spheres because of the following reasons. Firstly, the amount of produced PS fragments decreases with the reduction of the PS spheres. Secondly, at the very beginning of the etching process, the PS fragments from the neighboring PS spheres deposit on the same place, but the overlap of the deposition will disappear when the PS spheres are small enough (detailed in Fig. S2A of the ESI †). Therefore, the maximum thickness must exist during the etching process. According to our experimental results, the maximum thickness of the UR is observed when the etching duration is 9 min under this condition. But it is difficult to determine if it is the real maximum thickness of the UR, as indicated in Fig. S2B, it may exist when the etching time is in the range of 6 to 11 min.

To investigate the composition of the UR, we conducted XPS measurements. The carbon element of the following samples was characterized: Si after being etched for 3 min with oxygen plasma as the sample 1, i.e. the reference. Si assembled with PS after being etched for 3min with oxygen plasma, and then PS was removed as the sample 2.

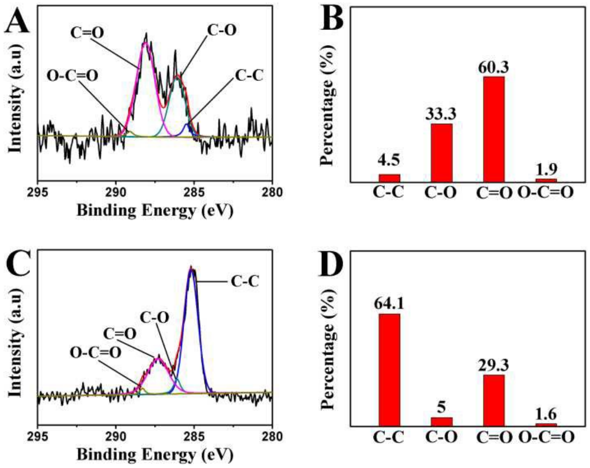

Fig. 3 XPS spectra of C1S region: the spectra (left column) and percentage of different functional groups (right column) for sample 1 (A, B), and sample 2 (C, D), respectively.

Fig. 3A and C present the fitting peaks for carbon functional groups of sample 1 and sample 2. The calculated percentage of the different carbon functional groups are accordingly shown in Fig. 3B and D. By fitting the C1S of reference, Fig. 3A identifies there are C-C (285.5eV), C-O (286.1eV), C=O (287.6eV) and O-C=O (289.8eV) groups. The percentage of C-C is 4.5%, C-O is 33.3%, C=O is 60.3%, and O-C=O is 1.9% (Fig. 3B). Comparing sample 2 with sample 1, they have the same kinds of functional groups (Fig. 3C), but the percentage of C-C increases from 4.5% to 64.1%, while C=O drops from 33.3% to 5% (Fig. 3D). The percentage variation of C-C between sample 1 and sample 2 could be caused by the formation of UR. In order to further identify the source of the resist layer, we calculated the carbon content of sample 1 and sample 2, the ratio of sample 2: sample 1 is 2.27:1. It means that the carbon content on Si with PS spheres is higher than that of bare Si after treating with oxygen plasma, which confirms that the redundant carbon on Si comes from PS spheres.

In order to test resist property of the UR for RIE, the sample (shown in Fig. 2D) was subjected to RIE for different time with SF_6 gas. Fig. 4A shows that a nanohole array was created when the sample was etched for 60 s. The average depth of the nanohole is ~24 nm (h), and the average diameter of the nanohole is ~369 nm (d) (Fig. 4B), which is almost same as the diameter of UR pattern (Fig. 2D). The results demonstrate the etching selectivity of Si to UR is higher. The correlation of the depth of nanohole and the etching duration is presented in Fig. 4C. It presents that the depth increases with extending the duration from 60 to 80 s. When extending the RIE duration to 80 s, the depth of the nanohole was increased to ~36 nm, and the diameter of the nanohole is ~363 nm, which also remained the same as that of the UR pattern. However, the surface became rougher, which indicates that the UR was slightly damaged by etching process. When the etching duration was further extended to 100 s, the depth nearly remained constant, but the diameter of the nanohole was ~398 nm, which was increased for ~9.6% (detailed in Fig. S3 of the ESI †). This should be caused by the isotropic chemical etching of SF_6. At the time, the UR has been destroyed absolutely, and the etching selectivity for Si to UR is 21:1.

To find out the difference of the spheres and the UR, we characterized the PS spheres and the UR with XPS. The peaks of C-C and C-O can be observed in both the spectra of the PS spheres (detailed in Fig. S4 of the ESI†) and the UR (Fig. 3C), the two peaks should respectively come from aliphatic and aromatic bond carbon, and the surface contamination. The peak of $\pi \rightarrow \pi^*$ should come from excitations in the benzene ring,[16] and it is too weak to be split from the spectra because of the lower content of benzene in the UR (Fig. 3C). But the peaks of C=O and O-C=O only can be found in Fig. 3C, which means that the UR is highly cross-linked. Therefore, the UR is much more dense and stable than PS spheres.

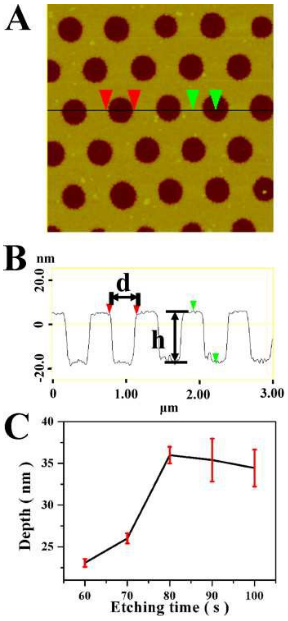

Fig. 4 (A) AFM topography and (B) Section analysis of the nanohole array created with SF_6 etching with resist pattern as mask. (C) Correlation of the average depth of nanoholes and etching duration. The resist pattern was created by etching for 9 min with oxygen plasma.

Furthermore, in order to study the blocking property of the UR to electrons, the sample (shown in Fig. 2D) was immersed into the mixed solution of silver nitrate, hydrogen peroxide, and hydrofluoric acid, site-selective electroless silver deposition will be produced (detailed in Fig. S5 of the ESI†). The result demonstrates the resist pattern can be applied as a site-selective template, and it is stable in the reaction solution.

Conclusions

In conclusion, we present a straightforward method to fabricate resist pattern based on the interaction of oxygen plasma and PS spheres within several minutes. In the fabrication process, PS spheres not only serve as template for resist patterning, but also provide PS fragments for the formation of the UR. The UR exhibits high etching selectivity to Si, meanwhile, it is a good template for site-selective redox reactions. This method could be applied for other polymers and substrates.

ACKNOWLEDGMENT

This work was supported by the National Natural Science Foundation of China (No. 21273092).

Notes and references

1 F. F. Wu, G. Shi, H. B. Xu, L. X. Liu, Y. D. Wang, D. P. Qi and N. Lu, *ACS Appl. Mater. Interfaces*, 2013, **5**, 12799-12803.

2 P. D. Ashby, D. L. Olynick, D. F. Ogletree and P. P. Naulleau, *Adv. Mater.*, 2015, **27**, 5813-5819.
3 Y. F. Chen, *Microelectron. Eng.*, 2015, **135**, 57-72.
4 F. F. Wu, L. X. Liu, L. Feng, D. R. Xu and N. Lu, *Nanoscale*, 2015, **7**, 13026-13032.
5 H. B. Xu, N. Lu, D. P. Qi, J. Y. Hao, L. G. Gao, B. Zhang and L. F. Chi, *Small*, 2008, **4**, 1972-1975.
6 C. Con, R. Dey, M. Ferguson, J. Zhang, R. Mansour, M. Yavuz and B. Cui, *Microelectron. Eng.*, 2012, **98**, 254-257.
7 K. H. Rasmussen, S. S. Keller, F. Jensen, A. M. Jorgensen and O. Hansen, *Microelectron. Eng.*, 2013, **112**, 35-40.
8 Y. C. Tseng, A. U. Mane, J. W. Elam and S. B. Darling, *Adv. Mater.*, 2012, **24**, 2608-2613.
9 L. O'Faolain, M. V. Kotlyar, N. Tripathi, R. Wilson and T. F. Krauss, *J. Vac. Sci. Technol. B*, 2006, **24**, 336-339.
10 K. M. Lim, S. Gupta, C. Ropp and E. Waks, *Microelectro. Eng.*, 2011, **88**, 994-998.
11 Y. C. Tseng, Q. Peng, L. E. Ocola, D. A. Czaplewski, J. W. Elam and S. B. Darling, *J. Mater. Chem.*, 2011, **21**, 11722-11725.
12 I. B. Baek, J. H. Yang, W. J. Cho, C. G. Ahn, K. Im and S. Lee, *J. Vac. Sci. Technol. B*, 2005, **23**, 3120-3123.
13 Y. Igaku, S. Matsui, H. Ishigaki, J. Fujita, M. Ishida, Y. Ochiai, H. Namatsu, M. Komuro and H. Hiroshima, *Jpn. J. Appl. Phys. 1*, 2002, **41**, 4198-4202.
14 G. M. Schmid, L. E. Carpenter and J. A. Liddle, *J. Vac. Sci. Technol. B*, 2004, **22**, 3497-3502.
15 A. J. M. Mackus, A. A. Bol and W. M. M. Kessels, *Nanoscale*, 2014, **6**, 10941-10960.
16 L. Wegewitz, A. Prowald, J. Meuthen, S. Dahle, O. Hofft, F. Endres and W. Maus-Friedrichs, *Phys. Chem. Chem. Phys.*, 2014, **16**, 18261-18267.

Graphical Abstract

An ultrathin resist pattern of high selectivity is fabricated based on plasma-polystyrene interaction within several minutes.